Chapter 3

Luminescence Characteristics of $Sr_3Al_2O_6:Eu^{3+}$ and $Sr_3Al_2O_6:Eu^{3+},Dy^{3+}$ phosphor

Creativity is inventing, experimenting, growing, taking risks, breaking rules, making mistakes, and having fun.
(Mary Lou Cook)

3.1. Introduction

Though the long after glow of strontium aluminates have been studied extensively, much of the research is focused on the new promises which this material shows when doped with various rare earth compounds. The role of rare earths is very important considering the wide variety of application prospects it shows. In recent years, the different phases of strontium aluminate doped with the rare earths have been developed like $Sr_2Al_6O_{11}:Eu^{2+}$, $Sr_4Al_{14}O_{25}:Eu^{2+}$ [1, 2, 3], $SrAl_2O_4:Eu^{2+}$, Dy^{3+} [4, 5, 6], $SrAl_{12}O_{19}:Eu^{2+}$, $SrAl_4O_7:Eu^{2+}$ [7, 8], etc. These phosphors are known as efficient green and blue emitters and for their long persistent properties. The nanocrystalline phosphor $SrAl_2O_4:Ce^{3+}$, Pr^{3+}, Tb^{3+} [9], has also been reported with rare earth dopant effect on the optical properties of this phosphor. As our interest is centered around developing a very strongly emitting phosphor rather than on temperature - dependent phase transformation, we have concentrated on this aspect in the present paper.

Europium doped strontium aluminate is mostly reported to have characteristic emission of europium in the divalent state; however, some of the papers also report the presence of europium in divalent as well as trivalent state when calcined up to 750-900°C [10,11]. In mid 1990's Matsuzawa et al. [12] found that introduction of another rare-earth ion, Dy^{3+}, as a co-activator in green emitting $SrAl_2O_4:Eu^{2+}$ (SRA) system amazingly prolonged the persistence from seconds to many hours, this made it important for many dark vision applications. Since then such co-doping has gained worldwide attention and extensive research work is being carried out on the family of aluminates to synthesize LP phosphor with different emission colours. In the present paper, we report on the preparation and the characterization of $Sr_3Al_2O_6$: Eu^{3+}, $Sr_3Al_2O_6$: Dy^{3+}, $Sr_3Al_2O_6$: Eu^{3+}, Dy^{3+}, their luminescence properties and the influence of co-dopants on the photoluminescence (PL) intensity of these phosphors.

Rare earth doped and co-doped alkaline earth aluminates with the formula $MAl_2O_4:Eu^{2+},RE^{3+}$ have been studied for their persistent nature because of their brighter, long persisting photoluminescence and chemical stability over sulfide based phosphors. The quantum efficiency (i.e. ratio of number of emitted photons to the number of absorbed photons) of these phosphors was reported to be much better than conventional $ZnS:Cu^{+}$ phosphor [13]. Such fascinating characteristics have opened up innumerable applications involving luminous paints for warning signs, escape route markings, ceramic products, decorative pieces, switches, sports equipments, toys etc.

The rare earth elements have had and still have a unique and important impact on our lives. The unfilled 4f electronic structure of the rare earth elements makes them have special properties in luminescence, magnetism and electronics, which could be used to develop many new materials for various applications such as phosphors, magnetic materials, hydrogen storage materials and catalysts [14]. Rare-earth-doped luminescent materials (i.e. phosphors) are known to emit at distinct and different wavelengths in the electromagnetic spectrum and have been widely used in color cathode ray tubes (CRT), tri-phosphor fluorescent lamps, X-ray intensifying screens and newly developed vacuum mercury-free lamps, as well as various types of displays such as plasma display panels, field emission displays and projection TVs [15]. Recently, breakthroughs in inorganic light emitting diodes (LEDs) technology [16,17] are significantly catalyzing the development of energy-efficient solid-state lighting (SSL) with long lifetime. Solid-state lighting technology has now already penetrated in a variety of specialty applications, in effect, LEDs have completely changed the "world of luminance", for example automobile brake lights, traffic signals, liquid crystal displays and mobile backlights, flashlights and all manner of architectural spotlights [18].

Doping of trivalent rare earths into the host can help and modify the emission characteristics of the phosphor. Doping forms an integral part of any material to be synthesized or the core area, be it semiconductors used in display or insulators like phosphor for the industry. Judicious use of the dopants enhances and sometimes changes the emission characteristics of the phosphor. Rare earth based research has been the backbone of the display industry and still the 4fn levels play significant role in enhancing and improving the industry with their charming and fascinating spectroscopic transitions. The rare earth studied for the present case was europium as it gives a lot of information about the host along with other useful information like environment of the host. This rare earth is the most studied and forms an integral part of many display devices, its transitions are very simple and give valuable information on the host environment. This rare earth can be doped in two forms viz divalent and trivalent, it requires inert or reducing atmosphere to get into the divalent state. The europium in divalent state has transitions from the 4f6 5d1 to lower state whereas for the trivalent state it is generally from the $^5D_0$, $^5D_1$ to the ground state at ^7F_J (where J = 0, 1, 2, 3, 4). Our interest in this work was to monitor and study trivalent europium, and to see what information it provides about the host in which it has been incorporated. The line emission makes it more appealing to

study this rare earth. All the line emissions resulting from the different transitions of the europium are not experimentally verified for example if the transition is from say:

$$^5D_0 \rightarrow {}^7F_2, \text{ where } J=2$$

Theoretically there have to be five lines of the europium for this state, as the stark splitting for this state is $2J+1 = 5$.

But the instances of the all the five splitting lines are not observed experimentally nor there are instances when the stark lines matches both theoretically as well as experimentally.

Europium is a well-known and thoroughly studied element in the lighting and displays areas [19–23]. According to electronic structure of ground state Eu^{2+} (4f7) is half filled 4f level and therefore, its stability is greater than that of Eu^{3+} (4f6). However, Eu^{3+} ion is also seen in well known red phosphor, $Y_2O_3:Eu^{3+}$. Therefore, europium can exist as Eu^{2+} or Eu^{3+} depending upon preparation condition, and very often host-structure decides the charge of europium. Eu^{3+} activated Y_2O_3, $LnBO_3$ (Ln La, Gd and Y) and YVO_4 find applications as a red component in low-pressure Hg lamps and television projection tubes. Whereas Eu^{2+}-doped $BaMgAl_{10}O_{17}$ blue phosphor find application mainly in low-pressure Hg lamp.

The emission spectrum of Eu^{3+} is usually sharp and atom like one, which indicates inert nature of host, i.e. host job is to hold Eu^{3+} without disturbing emission states, which is due to protection of 4f orbitals by 5s and 5p orbitals. However, position of emission wavelength varies very slightly with its coordination number. For example, Eu^{3+} in 6-coordination exhibits red orange emission at 611 nm, whereas Eu^{3+} in 9- and 12-coordination shows emission at 615 nm and at 625 nm, respectively.

With $Eu^{3+}:Sr_3Al_2O_6$, the dopant and host cation charges are different and therefore the dopant distribution can be investigated. When a dopant ion and host ion have a different valency, defects are created to maintain charge neutrality. To learn more about the luminescence of Eu, a study was initiated to prepare and characterize Eu^{3+}: $Sr_3Al_2O_6$, since this system contains a host ion with a different charge than the dopant ion. When there is a charge mismatch, defects occur to maintain overall charge neutrality.

The effective ionic radius of the Sr^{2+} and the rare earth doped in the $Sr_3Al_2O_6$ system in this thesis is given below in the tabular form:

Table 3.1: Comparison of effective ionic radii (Å)

Ions	Sr^{2+}	Tb^{3+}	Ce^{3+}	Eu^{3+}	Eu^{2+}
Effective ionic radii in different coordination	1.26	1.04	1.14	1.066	1.25

Figure 3.1. shows a partial energy level diagram of the Eu^{3+} ion in a solid host. Each energy level shown in Figure 3.1. can be split into 2J + 1 sublevels, and this fine structure is sensitive to the local crystalline field surrounding the Eu^{3+} ion. Therefore, distinct spectra arise from the Eu^{3+} ions in different crystallographic cation sites.

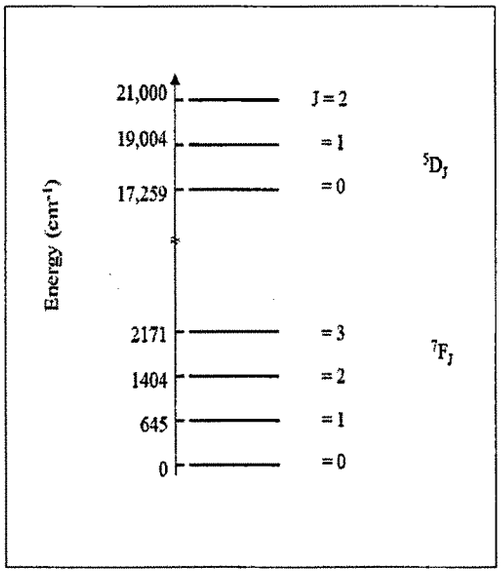

Figure 3.1. Partial energy level diagram of the Eu^{3+} ion in solids. Each level can be split into 2J + 1 sublevels.

The lanthanides have a well-documented history in studies of luminescence primarily for the fact that the f-f transitions produce narrow lines. Since the 4f electrons of the lanthanides are shielded from perturbations with the lattice by the outer 5s and 5p electrons, the 4f orbitals retain their hydrogenic character, resulting in sharp transitions between the 4f levels. A thorough review of the early spectroscopic work of lanthanides is provided by Dieke [24]. Current work on lanthanide luminescence is diverse in scope due to both fundamental interest and potential applications. In addition to the technologically important applications, lanthanides serve as a probe of their local

chemical environment. As mentioned in the foregoing paragraph, the 4f transitions are sharp and the 4f orbitals are sensitive to their local crystal field.

Consequently, the J-multiplet levels are split and the splitting pattern is dependent on the strength of the crystal field and local site symmetry. Therefore, the luminescent spectra consist of lines that are characteristic of the local chemical environment.

In the case of Eu^{3+} ions, the main emission lines occur between the $^5D_0$ level and ^7F_J multiplets. Their narrow emission lines have low intensity, because they are parity and spin forbidden. The oscillator strengths of absorption to the excited states of Eu^{3+} ions, as for other rare earth ions, are of the order of magnitude 10^{-5}–10^{-6} [25].

The $^5D_0 \rightarrow {}^7F_J$ emission is very suitable for surveying the transition probabilities of sharp spectral features in rare earths. If a rare-earth ion occupies a site with inversion symmetry in a crystal lattice, the optical transitions between 4f*n* levels are strictly forbidden as electric-dipole transitions (due to the parity selection rule). They can only occur as magnetic-dipole transitions, which obey the selection rule $\Delta J = 0, \pm 1$ ($J = 0$ to $J = 0$ being forbidden), or as vibronic electric dipole transitions. If there is no inversion symmetry at the site of a rare-earth ion, the odd crystal field components can mix opposite-parity states into 4f *n*-configurational levels. Electric-dipole transitions are now no longer strictly forbidden and appear as weak lines in the spectra, the so-called forced electric-dipole transitions. Some transitions, viz. those with $\Delta J = 0, \pm 2$, are hypersensitive to this effect. Even for small deviations from inversion symmetry, they appear dominantly in the spectrum [26].

3.2. Experimental

All the phosphor samples were prepared by the reflux method. The starting materials taken were strontium nitrate, aluminium nitrate and the rare earths in the nitrate form. All of them were acquired from S.D. Fine Chemicals with rare earths of purity 99.9%. The first set of the samples was prepared by doping the Europium nitrate in the host matrix. The powders were weighed according to the nominal composition of $Sr(NO_3)_2$+$Al(NO_3)_3.9H_2O$+ x $Eu(NO_3)_3$ (x = 0%, 1%, 1.5%, 2%). Second set of samples were prepared with dysprosium as dopant with composition as $Sr(NO_3)_2$+$Al(NO_3)_3.9H_2O$+ y $Dy(NO_3)_3$ (y = 0%, 0.025%, 0.5%, 1%, 1.5%, 2%). Also a third set of samples were prepared doped and co-doped with europium and dysprosium, respectively, i.e. $Sr(NO_3)_2$+$Al(NO_3)_3.9H_2O$+ 1% $Eu(NO_3)_3$+ y $Dy(NO_3)_3$ (y = 0%, 0.1%,0.2%,0.3%, 0.5%, 2%).

The starting materials strontium and aluminum nitrates were taken in 1:2 proportions and dissolved in the appropriate amount of distilled water and kept for stirring. Thereafter the rare earths compounds with different concentrations were mixed to the above solution. Citric acid and ethylene glycol were added to the solution after one hour of constant stirring. The resulting gel was set for refluxing at 100°C for 3 hours. The gel thus obtained, was kept for drying in an oven maintained at 100°C for 10 hours. The yellowish gel then transformed into a fluffy material. It was then kept for firing at a temperature maintained at 900°C in a furnace for 16 hours in air. The white powder obtained on firing, was ground using an agate mortar and pestle and was then subjected to various characterizations. The main function of citric acid and ethylene glycol is to provide a polymeric network to hinder cations mobility, which maintans local stoichiometry and minimizes precipitation of unwanted phase. An added feature of having an organic resin as a carrier is the potential heat of combustion produced during calcinations [27].

Phase identification of the powders was carried out by the X-ray powder diffraction using RIGAKU D'MAX III Diffractometer having Cu Kα radiation. The photoluminescence (Emission and Excitation spectra) were recorded at room temperature using spectrofluorophotometer RF-5301 PC of SHIMADZU make. The thermoluminescence glow curve of all the samples were recorded using Nucleonix make TL reader with a heating rate of 7.5 °C/s. For measuring the thermoluminescence glow curve all the samples were first irradiated with Beta rays from a Sr-90 source of 50 mCurie strength.

3.3. Results and Discussion

3.3.1. X-ray diffraction (XRD) studies

In order to determine the crystal structure, phase purity, chemical nature and homogeneity of the phosphors, X-ray diffraction (XRD) analysis was carried out. Figure 3.2. shows X-ray diffraction (XRD) pattern of the $Sr_3Al_2O_6:Eu^{3+}(1\%),Dy^{3+}(0.1\%)$ phosphor. From the XRD pattern analysis it was found that the prominent phase formed is $Sr_3Al_2O_6$. The $Sr_3Al_2O_6$ phase belongs to the space group pa3 having a cubic crystalline structure (JCPDS card no. - 24-1187). Where few $SrAl_4O_7$ peaks were also observed, the peaks representing $SrAl_2O_4$ were very weak. All the samples followed the same XRD pattern.

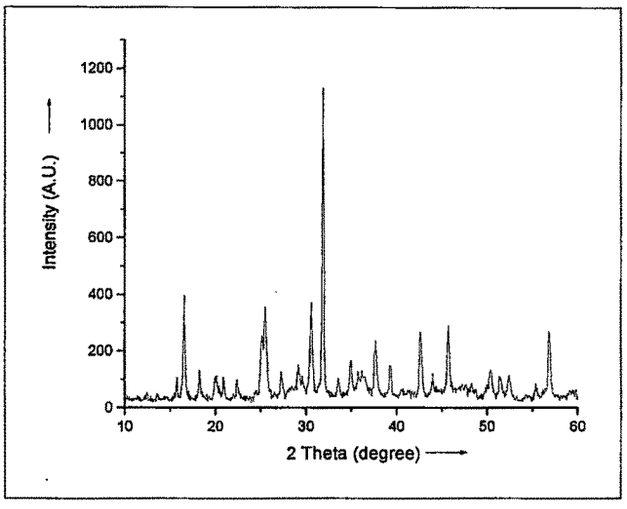

Figure 3.2. X-ray diffraction pattern of $Sr_3Al_2O_6$:Eu^{3+}(1%),Dy^{3+}(0.1%)

3.3.2. Photoluminescence (PL) characteristics

The excitation and emission spectra of $Sr_3Al_2O_6$: x Eu, (where x = 0%, 1%, 1.5%, 2%) were measured at room temperature and are shown in Figure – 3.3 A & B respectively. The emission spectra were recorded for all the phosphors after exciting them with 254 nm wavelength. The undoped $Sr_3Al_2O_6$ material does not show any luminescence but the emission spectra of europium doped material shows luminescence in the wavelength range from 580-620 nm. The $Sr_3Al_2O_6$: Eu^{3+} phosphor exhibit narrow emission at 580 nm, 592 nm, 595 nm, 613 nm, 617 nm instead of characteristic 520 nm emission which is the case for divalent europium. One can also observe from the Figure-3.3(B) that as the europium concentration increased from 1% to 2% the intensity of the lines at the respective wavelengths also goes on increasing. It is well known that the luminescent intensity is related to the average distance between luminescent centers. With the doping concentration increase, the distance between active ions decreases. The interaction between active ions will cause concentration quenching when the distance is short enough. Therefore, the homogeneous distribution of active ions in host is essential to acquire highly doped phosphors without concentration quenching. The sol–gel combustion method provides a more homogeneous environment, and enhances the distribution of Eu^{3+} in the host. The good distribution of Eu^{3+} activators could result in an increase in the emission intensity and quenching concentration. Such unexpected trivalent emission from $Sr_3Al_2O_6$: Eu^{3+} materials were also observed by Song et. al. [10], wherein

they considered $Sr_3Al_2O_6$ to be an intermediate phase at 900 °C alongwith the presence of $SrAl_2O_4$ and $SrAl_4O_7$. As the temperature was increased above 1200 °C the $Sr_3Al_2O_6$ and $SrAl_4O_7$ transforms into $SrAl_2O_4$. Song et. al. also stated that the Eu^{3+} ions stabilized at the $Sr_3Al_2O_6$ sites only. At the elevated temperatures alongwith the transformation of $Sr_3Al_2O_6$ into $SrAl_2O_4$ the trivalent europium (Eu^{3+}) also was converted into divalent (Eu^{2+}) form. This observation of trivalent europium (Eu^{3+}) emission alongwith divalent europium (Eu^{2+}) is also reported by Yun Liu et al. [11] at 750 - 1000 °C. The authors have further reported that the host $Sr_3Al_2O_6$ was not responsible for the emission from trivalent europium but it was $SrAl_2O_4$ that was responsible for the emission due to the lack of inversion symmetry. The Calvert and Danby [28] that if the alkaline earth nitrates are used as starting material then the probability of europium, acting as activator, added enters the lattice predominantly in trivalent form, perhaps due to the oxidizing nature of the HNO_3. In our synthesis technique also we are using strontium nitrate as a starting material which must be responsible for stabilization of the Eu^{3+} in the lattice. This shows that Eu can replace easily Sr^{2+} ion substitutionally in trivalent state rather than in divalent state. This may due to the fact that the ionic radius of Eu^{2+} (1.25Å) is near about equal to that of Sr^{2+} (1.26Å) whereas the ionic radius of Eu^{3+} (1.066Å) is slightly lower. The charge transfer band of Eu^{3+} located at 210 nm [29] overlaps quite reasonably with the main mercury emission at 254 nm, making direct sensitization of the phosphor feasible.

Figure 3.3 (B) shows very intense emission spectra of trivalent europium ion. Further the high intensity ratio for the two fluorescence transitions mainly $^5D_0 \rightarrow {}^7F_2$ and $^5D_0 \rightarrow {}^7F_1$ indicates that the Eu^{3+} site is closer to the inversion symmetry [30,31,32] and is also attributed to $Sr_3Al_2O_6$ host lattice as there is no evidence of $SrAl_2O_4$ being present. We are at variance with the observations of Yun Liu et. al., on this point as our XRD pattern clearly shows the $Sr_3Al_2O_6$ as the prominent phase and our results are in agreement with those reported by Song et. al. [10]. Moreover the highly intense emission of the europium in the $Sr_3Al_2O_6$ is clearly seen in the Figure 3.3(B) resulting transitions from $^5D_0 \rightarrow {}^7F_J$ (J = 0, 1, 2) and no transition is observed which could be due to the characteristic of divalent europium (Eu^{2+}) i.e. from $^4F_6{}^5D_1 \rightarrow {}^4F_7$.

Luminescence originating from electronic transition between 4*f* levels is predominantly due to electric and magnetic dipole interactions. In principle, electric dipole moment of *f-f* transitions in free 4*f* ions are forbidden by the Laporte's selection rule. However, such transitions are allowed when spin-orbit interaction occurs. This interaction is formed by the odd crystal-field terms [33], that is to say terms that change sign on inversion with

respect to rare-earth ions. The selection rule in this case is $|\Delta J| \leq 6$ (except for $0 \rightarrow 0$, $0 \rightarrow 1$, $0 \rightarrow 3$, $0 \rightarrow 5$). Typical examples are the transitions from ^5D_J to ^7F_J levels of the Eu^{3+}, $^4F_{3/2}$ to ^4I_J of Nd^{3+} and $^5D_4$ to ^5F_J of Dy^{4+}.

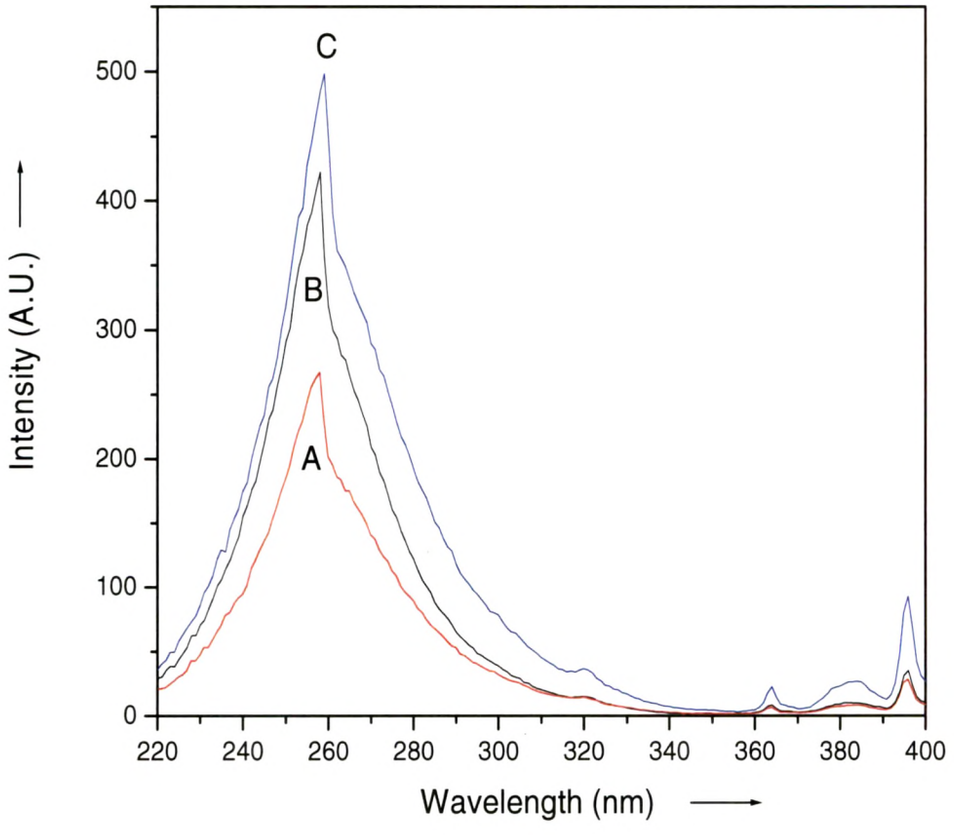

Figure 3.3.A . Excitation Spectra of $Sr_3Al_2O_6:Eu^{3+}$.
Emission : 613nm.
Curve A = $Sr_3Al_2O_6$: 1%Eu;
B = $Sr_3Al_2O_6$: 1.5%Eu;
C = $Sr_3Al_2O_6$: 2 %Eu.

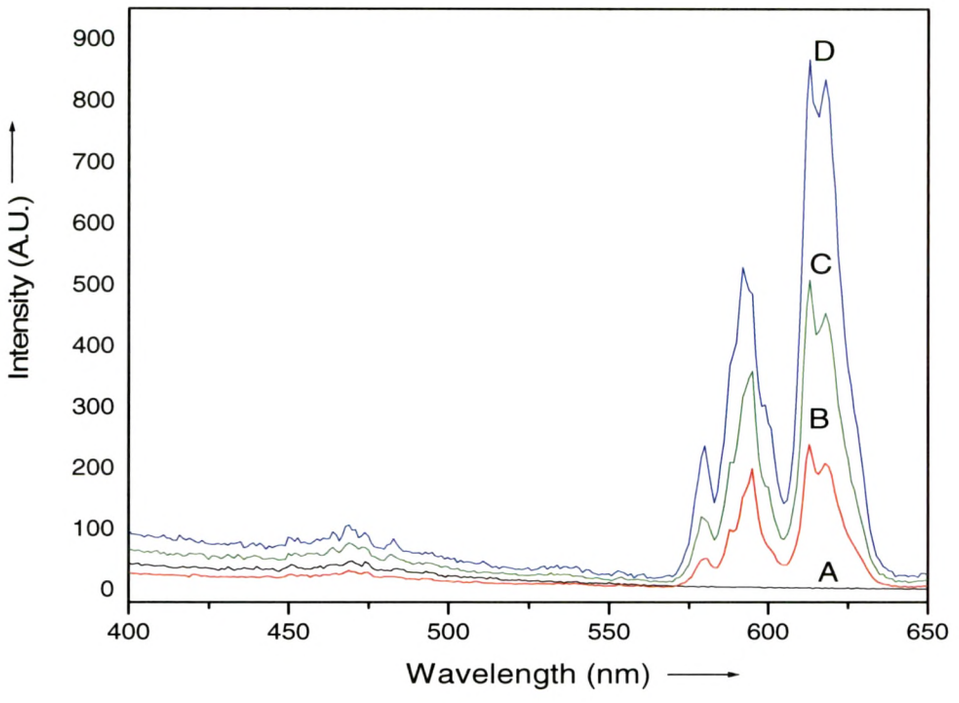

Figure 3.3.B. Emission Spectra of $Sr_3Al_2O_6:Eu^{3+}$. Excitation:254nm.
Curve A = $Sr_3Al_2O_6$: 0%Eu;
B = $Sr_3Al_2O_6$: 1%Eu;
C = $Sr_3Al_2O_6$: 1.5%Eu;
D = $Sr_3Al_2O_6$: 2%Eu.

Table 3.2: Photoluminescence peak intensity of $Sr_3Al_2O_6:Eu^{3+}$ phosphor

Sample Code	Name of the sample	PL wavelength (nm)	PL peak intensity (A.U.)
A	$Sr_3Al_2O_6$: 0%Eu	--	--
B	$Sr_3Al_2O_6$: 1%Eu	580, 592, 612, 617	54,202,240, 210
C	$Sr_3Al_2O_6$: 1.5%Eu	580, 592, 612, 617	121,361,510,460
D	$Sr_3Al_2O_6$: 2%Eu	580, 592, 612, 617	236,525,866,836

Figure 3.4 shows the excitation spectra of $Sr_3Al_2O_6$: (1%)Eu^{3+} phosphor in the 300-550nm range. The emission wavelength at 613nm shows sharp lines in the spectra corresponding to the direct excitation of the Eu^{3+} ground state to higher levels of the 4f-manifold. The transitions at the $^7F_{0,1} \rightarrow {}^5D_2$ are clearly seen at 466nm. These lines were also reported in the Eu^{3+}doped $LaPO_4$ material by R.Y.Wang [30]. We observed the ^7F

$_{0,1}\rightarrow{}^5D_4$, $^7F_{0,1}\rightarrow{}^5G_J$,$^5L_7$ and $^7F_{0,1}\rightarrow{}^5L_6$ along with $^7F_{0,1}\rightarrow{}^5D_1$ transitions at 364nm, 384nm, 396nm and 533nm respectively.

We shall first consider charge transfer state (CTS), where electrons in the neighbouring anions are transferred to a 4*f* orbital. This is an allowed transition thus strong optical absorption occurs. The most common rare-earth ion showing this phenomenon is Eu^{3+}. In the emission process of the Eu^{3+} ion the charge transfer level from anion of host lattice plays in part, since the ions decay from the CTS via number of 4*f* levels to ^5D level, from which the ground state is reached by the emission of radiation.

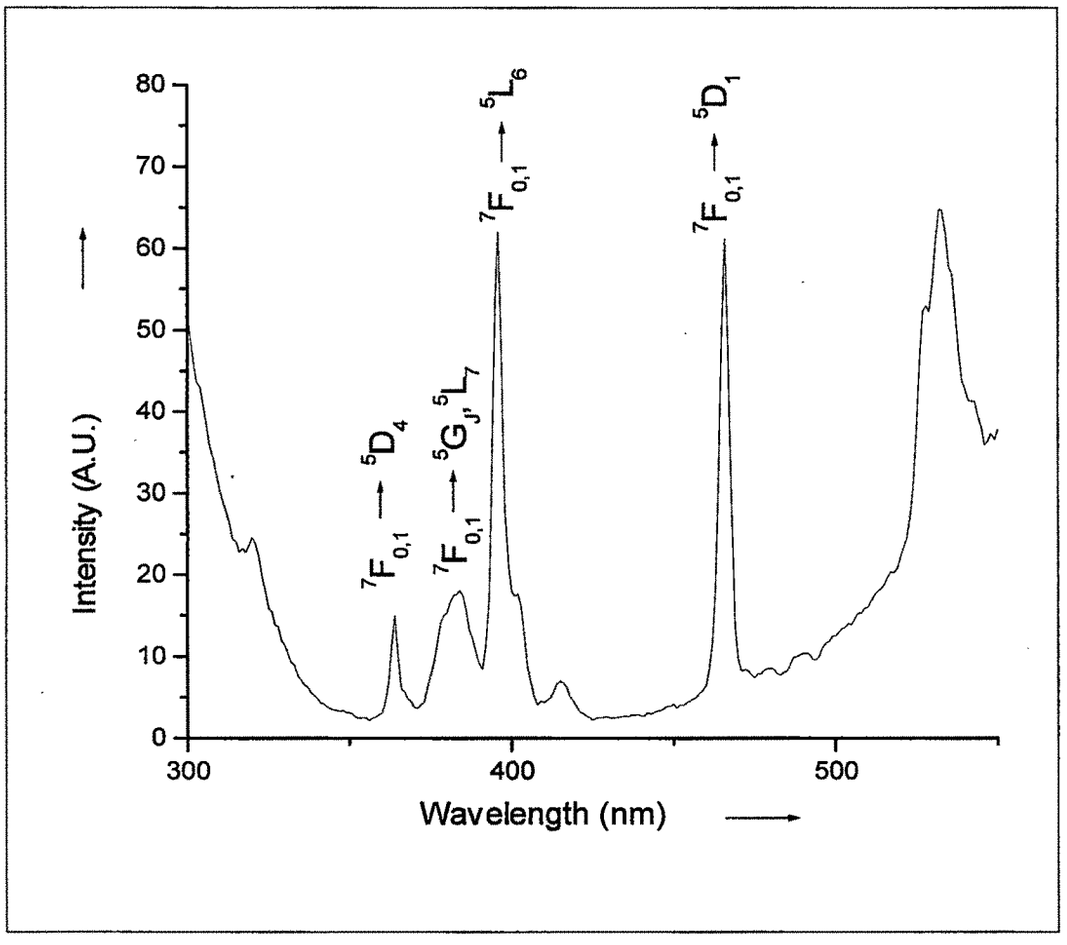

Figure 3.4. Excitation Spectra of $Sr_3Al_2O_6:Eu^{3+}$ in the range 300-550nm at room temperature. Emission:613nm.

The figures 3.5 A & B shows the excitation and emission spectra of the $Sr_3Al_2O_6$: Eu^{3+},Dy^{3+} phosphors. Curve-A in the figure 3.5 represents the emission spectra of $Sr_3Al_2O_6$: (0.5%) Dy^{3+} phosphor, surprisingly dysprosium doping in the $Sr_3Al_2O_6$ has not yielded any luminescence. Up till now $SrAl_2O_4$: Eu^{2+}, Dy^{3+} has been reported as an excellent long persistent phosphor [4, 5, 6], on the other hand $Sr_3Al_2O_6$: Eu^{2+}, Dy^{3+} phosphor has been reported as an excellent mechanoluminescent phosphor emitting green light [34,35]. The Table 3.3 depicts the doping and co-doping concentrations in all the samples. On doping Dy^{3+} in $Sr_3Al_2O_6$: Eu^{3+} we got the emission in the red region of the visible spectrum. As the concentration of Dy^{3+} was increased from 0.1% to 2% the emission of Eu^{3+} i.e. in the red region kept decreasing due to the energy dissipation during the Eu-Dy energy transfer. Based on the fact that the emission due to Dy^{3+} is not observed and still the addition of Dy^{3+} decreases the emission intensity of Eu^{3+}, it can be correlated to the presence of the major phase of $Sr_3Al_2O_6$ in the host material rather than that of $SrAl_2O_4$ thereby showing the quenching effect due to addition of Dy^{3+}.

In other rare-earth ions such as Dy^{3+} the CTS energy is high, in accordance with the fact that it is not easily reduced. Thus, direct UV excitation is not effective. It is most probable that excitation by host complex brings about transition from $^4F_{9/2}$ $^6H_{15/2}$ and $^6F_{15/2}$ $^6F_{11/2}$, example $Y(P,V)O_4$:Dy^{3+} [36,37].

Mainly, the luminescence observed from all the dopant ions is because of transfer of energy from one ion to another. When this transfer takes place between ions of the same species, it is called energy migration. If the energy migration is high it increases the probability that the optical excitation is trapped at defects or impurity sites, enhancing non-radiative relaxation. This causes concentration quenching because an increase in the activator concentration encourages such nonradiative processes [38,39]. As a result, the excitation energy diffuses from ion to ion before it is trapped and leads to emission. On the other hand, a decrease in the activator concentration decreases the energy stored by the ions. Hence, an optimum amount of activator concentration is a must to get an efficient phosphor.

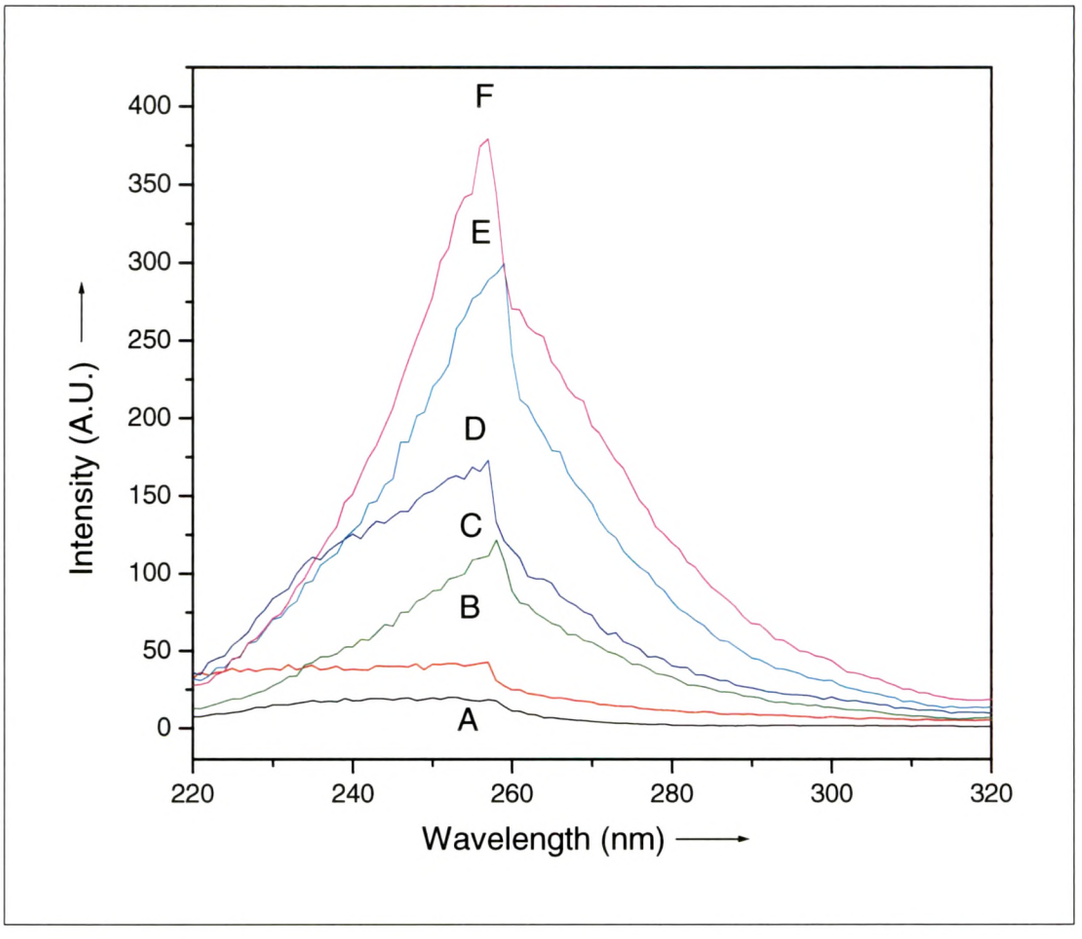

Figure 3.5.A. Excitation spectra of $Sr_3Al_2O_6:Eu^{3+},Dy^{3+}$.
Emission: 613nm.
Curve A = $Sr_3Al_2O_6$: 1%Eu,2%Dy;
B = $Sr_3Al_2O_6$: 0%Eu,0.5%Dy;
C = $Sr_3Al_2O_6$: 1%Eu,0.5%Dy;
D = $Sr_3Al_2O_6$: 1%Eu,0.3%Dy;
E = $Sr_3Al_2O_6$: 1%Eu,0.2%Dy;
F = $Sr_3Al_2O_6$: 1%Eu,0.1%Dy.

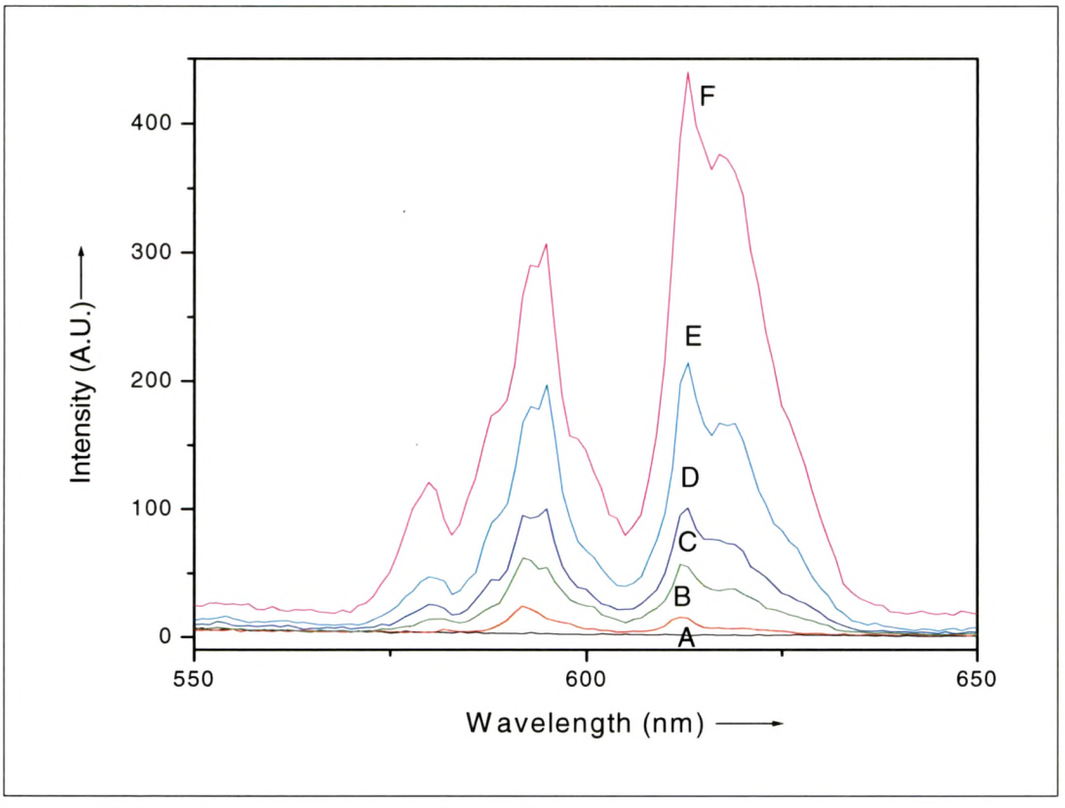

Figure 3.5.B. Emission spectra of $Sr_3Al_2O_6:Eu^{3+},Dy^{3+}$. Excitation: 254nm.
Curve A = $Sr_3Al_2O_6$: 0%Eu,0.5%Dy;
B = $Sr_3Al_2O_6$: 1%Eu,2%Dy;
C = $Sr_3Al_2O_6$: 1%Eu,0.5%Dy;
D = $Sr_3Al_2O_6$: 1%Eu,0.3%Dy;
E = $Sr_3Al_2O_6$: 1%Eu,0.2%Dy;
F = $Sr_3Al_2O_6$: 1%Eu,0.1%Dy.

Table 3.3: Photoluminescence peak intensity of $Sr_3Al_2O_6:Eu^{3+},Dy^{3+}$ phosphor

Sample Code	Name of the sample	PL wavelength (nm)	PL peak intensity (A.U.)
A	$Sr_3Al_2O_6$: 0%Eu,0.5%Dy	--	--
B	$Sr_3Al_2O_6$: 1%Eu,2%Dy	580,592, 612,	6,23,15
C	$Sr_3Al_2O_6$: 1%Eu,0.5%Dy	580,592, 595,612, 617	15,62,55,58,38
D	$Sr_3Al_2O_6$: 1%Eu,0.3%Dy	580, 592,595, 612, 617	25,97,100,101,75
E	$Sr_3Al_2O_6$: 1%Eu,0.2%Dy	580, 592,595, 612, 617	49,181,199,212,16 6
F	$Sr_3Al_2O_6$: 1%Eu,0.1%Dy	580, 592,595, 612, 617	119,289,308,438,3 75

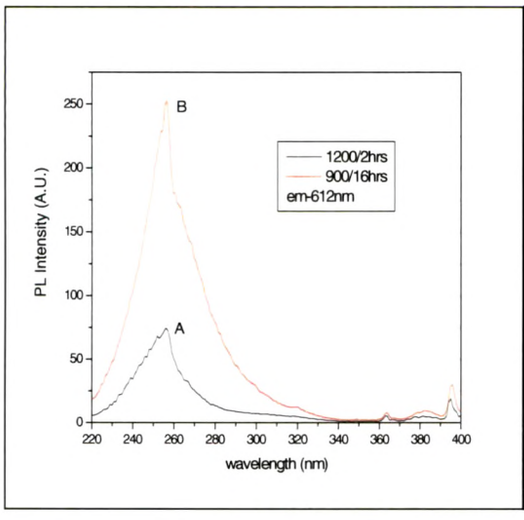

Figure 3.6.A. PL excitation spectra of $Sr_3Al_2O_6:Eu^{3+}$ (1%), Dy^{3+} (0.1%).
Emission : 613nm.
Curve A = annealed at 1200 °C/16 hrs ;
B = annealed at 900 °C/16 hrs.

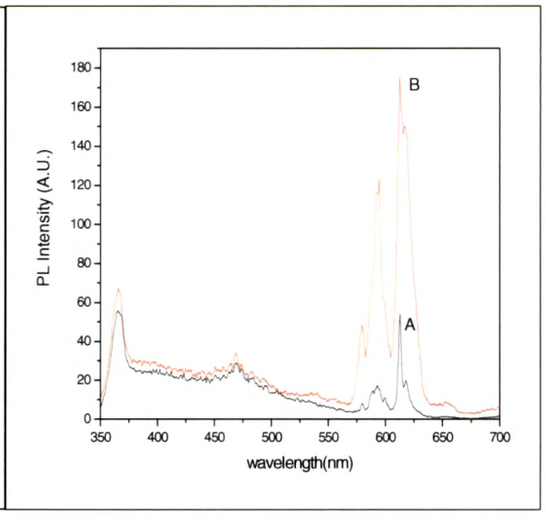

Figure 3.6.B. PL emission spectra of $Sr_3Al_2O_6:Eu^{3+}$ (1%), Dy^{3+} (0.1%).
Excitation : 254nm.
Curve A = annealed at 1200 °C/16 hrs ;
B = annealed at 900 °C/16 hrs.

Figure 3.6 A & B represents the PL excitation and emission spectra of $Sr_3Al_2O_6:Eu^{3+}$ (1%), Dy^{3+} (0.1%) phosphor annealed at 1200 °C and 900 °C for 16 hours. The strongest emission peak at 613nm is due to forced electric dipole transition of $^5D_0$- $^7F_2$. It is characteristic red emission of Eu^{3+}. The intensity ratio of $^5D_0$- $^7F_2$ to $^5D_0$- $^7F_1$ can be viewed as a clue concerning the nature of the local surroundings of the luminescent center and its symmetry [5]. It can be seen that the ratio between 613nm vs. 595nm decreases with increase in sintering temperature. This reflects change of the local surroundings for the luminescent center during the transformation from $Sr_3Al_2O_6$ to $SrAl_2O_4$ phase. Thus it can be observed that the europium in the trivalent form can be incorporated only in the $Sr_3Al_2O_6$ phase which occurs when the phosphor is annealed to 900 °C for 16 hours. As it can be observed from the XRD pattern obtained for different annealing temperatures that the SrO :Al_2O_3 system forms different phases at different annealing temperartures. The phosphor annealed at 1200°C/16hrs shows the traces of $SrAl_2O_4$, $SrAl_4O_7$ phase. The prescence of $Sr_3Al_2O_6$ phase at 1200°C is very meagre, hence the europium which stabilizes in the trivalent form cannot get incorporated in the system. So the prescence of

other phases reduces the PL emission intensity of Eu^{3+} ion in this system. Hence to get the intense emission of Eu^{3+} in this system the $Sr_3Al_2O_6$ phase should be dominant.

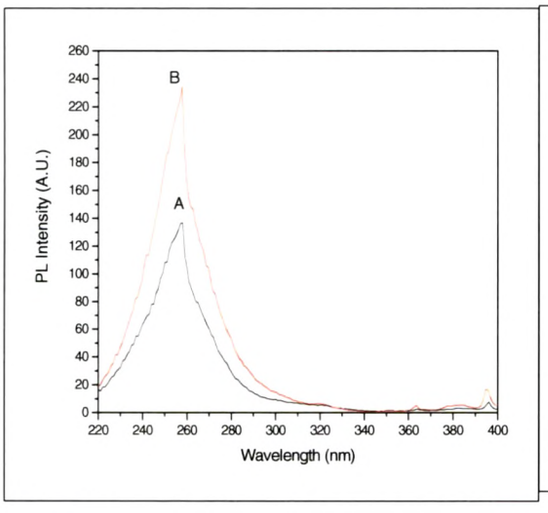

Figure: 3.7.A. PL excitation spectra of $Sr_3Al_2O_6:Eu^{3+}$ (1%). Emission : 613nm. Curve A = $Sr_3Al_2O_6$ annealed in an reducing atmosphere at 1200 °C/16 hrs ; B = $Sr_3Al_2O_6$ annealed in an reducing atmosphere at 900 °C/16 hrs.

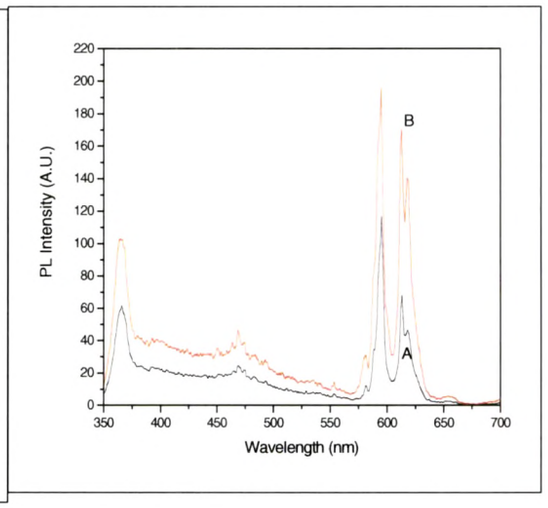

Figure: 3.7.B. PL excitation spectra of $Sr_3Al_2O_6:Eu^{3+}$ (1%). Excitation : 254nm. Curve A = $Sr_3Al_2O_6$ annealed in an reducing atmosphere at 1200 °C/16 hrs ; B = $Sr_3Al_2O_6$ annealed in an reducing atmosphere at 900 °C/16 hrs.

Figure 3.7 A & B represents the PL excitation and emission spectra of the $Sr_3Al_2O_6:Eu^{3+}$(1%) phosphor annealed in a reducing atmosphere at 1200 °C/16 hrs and 900 °C/16 hrs.

Presence of rare-earth, Eu^{3+} was confirmed by fluorescence spectra. Excitation wavelength was always 254 nm. It shows doublet in the region 610–618 nm and another doublet in the region 590–595 nm. The former doublet is due to electric dipole transition whereas the latter is due to magnetic dipole transition. The intensity of the doublet due to magnetic dipole transition is slightly higher than that of doublet due to electric dipole transition. It is normal that either electric dipole transition or magnetic dipole transition predominates in most of the oxide phosphors. But, here the observation is quite different since our earlier results, obtained when annealed in an air, show the dominance of electric dipole transitions. Hence the phosphor prepared in the reducing atmosphere show different site symmetry closer to Eu^{3+} site. From this observation, we can say that because of observation of both the transition contribute both the color rendering index

and lumen output. Therefore, these phosphors are potential for fluorescent lamp phosphor to get higher lumen output and greater color rendering index.

3.3.3. Thermally Stimulated Luminescence characteristics

The phosphors were subjected to the Thermally Stimulated Luminescence (TSL) study to ascertain the defects present in the synthesized compounds. The thermoluminescence glow curve of the $Sr_3Al_2O_6$, $Sr_3Al_2O_6$:Eu^{3+} (1%) and $Sr_3Al_2O_6$:Eu^{3+},Dy^{3+} (1%, 0.1%) samples were obtained in the temperature range between room temperature to 450 °C. A test dose of 10kGy from a beta source (Sr-90) of 50 mCurie strength was given to all the samples. The thermoluminescence glow curves were measured for heating rate of 7.5 °C /sec. Figure 3.8 shows the TL glow curves of beta irradiated $Sr_3Al_2O_6$, $Sr_3Al_2O_6$:Eu^{3+} (1%) and $Sr_3Al_2O_6$:Eu^{3+},Dy^{3+} (1%, 0.1%) phosphors.

The host lattice viz. $Sr_3Al_2O_6$ did not show any glow peaks while $Sr_3Al_2O_6$: Eu^{3+} (1%) sample showed a very weak glow peak at around 194 °C. The glow curve for $Sr_3Al_2O_6$: Eu^{3+},Dy^{3+} (1%, 0.1%) (Figure 3.8 curve-C) however showed an intense glow peak at the same temperature of 194 °C. The traps in the $Sr_3Al_2O_6$, $Sr_3Al_2O_6$: Eu^{3+} seems to be very low due to lack of trapping levels present in the compound but on the doping of dysprosium in $Sr_3Al_2O_6$:Eu^{3+} the electron concentration increases and the traps are formed, though at deep levels. The $Sr_3Al_2O_6$: Eu^{3+},Dy^{3+} (1%, 0.1%) material was also illuminated with a UV lamp of 365nm wavelength for 30 minutes, but no thermoluminescence was observed. The trap depth of the β-irradiated $Sr_3Al_2O_6$: Eu^{3+}, Dy^{3+} (1%, 0.1%) (Figure 3.8 curve C) sample were calculated by Hoogenstraten equation and also by Chen's equation. We found that the trap depth calculated by Hoogenstraten equation [6, 11] was 0.17 eV and by Chen's equation [40] was 0.87 eV. The significantly large difference in the values of trap depth is attributed to the Hoogenstraten equation being very approximate in estimating the trap depth value. The calculated trap depth in the $Sr_3Al_2O_6$: Eu^{3+},Dy^{3+} (1%, 0.1%) is too deep to give phosphorescence at room temperature. This could be the main reason for the absence of long afterglow even after UV illumination. The TL glow curve of $Sr_3Al_2O_6$:Eu^{3+},Dy^{3+} was also studied by Morito et. al[34] in the temperature ranging from room temperature to 250 °C and they found it to be very weak compared to the $SrAl_2O_4$: Eu^{3+},Dy^{3+} and $SrAl_4O_7$: Eu^{3+},Dy^{3+}.

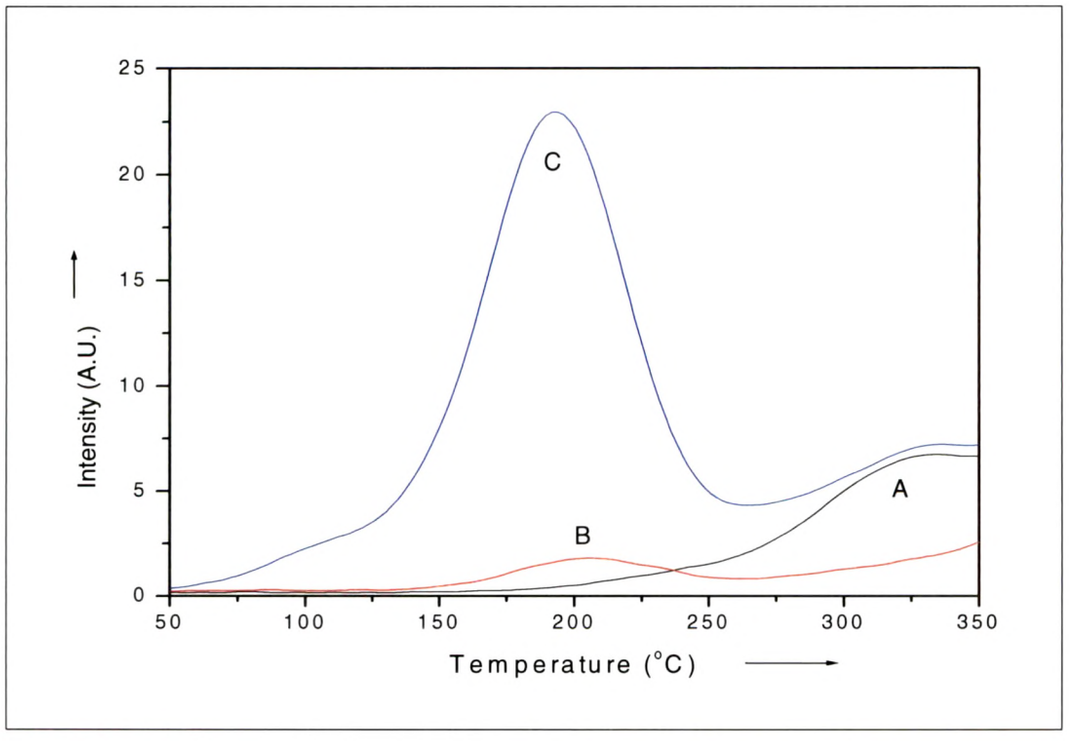

Figure: 3.8. TL Glow Curve of the samples;
A = $Sr_3Al_2O_6$;
B = $Sr_3Al_2O_6$:Eu^{3+} (1%);
C = $Sr_3Al_2O_6$:Eu^{3+} (1%), Dy^{3+} (0.1%).

The PL excitation and emission spectrum of the gamma as well as beta irradiated $Sr_3Al_2O_6$:Eu^{3+} (1%) phosphor was measured, to identify any change in the charge state of Eu^{3+} after irradiation. The phosphor was irradiated to 1kGy Gamma rays and then its PL spectrum was measured. The remarkable reduction in the emission intensity was observed whereas no trace of Eu^{2+} fluoroscence was observed. This shows that after irradiation to gamma rays there is no change in the charge state of the Eu^{3+} occurs.

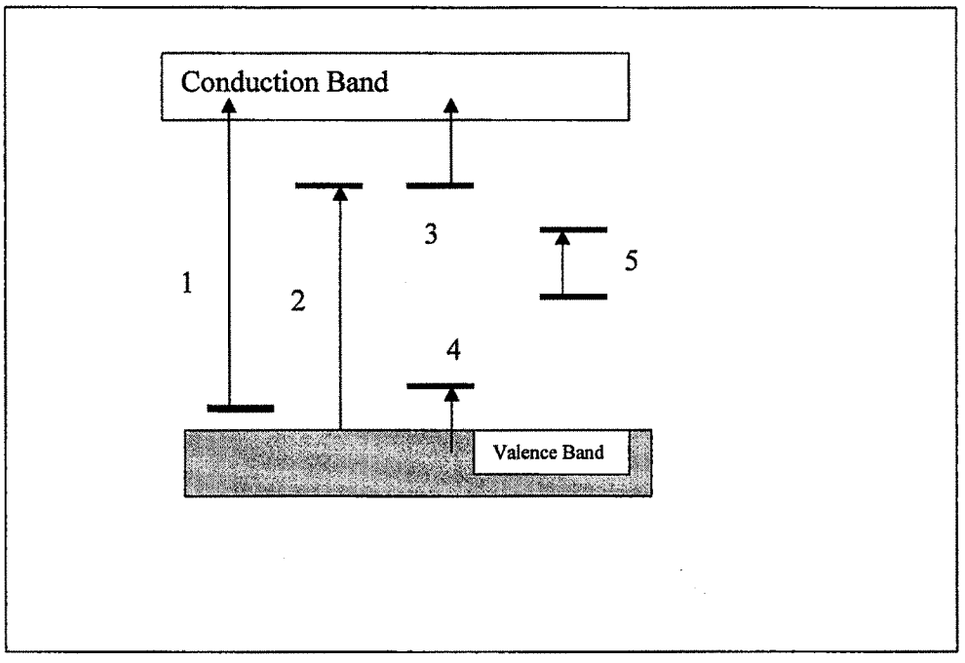

Figure 3.9. Schematic representation of the possible transitions in the insulator 1 & 2. defect ionization; 3 & 4. trap ionization; 5. internal intra-center transition.

The above figure shows the different types of the transitions in the insulators. Where the transitions 1 & 2, 3 & 4 are responsible for the thermoluminescence glow peak formation. In any material the formation of the TL glow peaks is depend on the presence of the defects that create traps and recombination center in the host lattice. Generally these defects are formed by addition of the dopant in the matrix or it may form due to presence of impurities and different phases.

The transition 5 depicted in the figure shows the transition responsible for the PL emission and absorption. The luminescence emitted from the following absorption of light by an internal transition as shown in 5. Since this does not involve transport of charge from one defect site to another such transitions do not affect the TL signal.

All these types of transitions are observed in the $Sr_3Al_2O_6$:Eu,Dy phosphor. The photoluminescence and Thermoluminescence study of this phosphor is published in the Material Research Bulletin [41].

3.4. References

[1] B.Smets, J.Rutten, G.Hoeks, J. Electrochem. Soc., 136 (1989) 2119.

[2] Wang Minquan, Dong Wang, Lu Guanglie, Materials science and Engineering, B57 (1998) 18.

[3] Yuanhua Lin, Zilong Tang, Zhongtai Zhang, Materials Letters, 51 (2001) 14.

[4] Tianyou Peng, Liu Huajun, Huanping Yang, Chunhua Yan, Materials Chemistry and Physics, 85 (2004) 68.

[5] Yuanhua Lin, Zhongtai Zhang, Zilong Pang, Junying Zhang, Zishan Zheng, Xiao Lu, Materials Chemistry and Physics, 70 (2001) 156.

[6] Abanti Nag, T. R. N. Kutty, Journal of Alloys and Compounds, 354 (2003) 221.

[7] Mickael Capron and Andre Douy, J. Am. Ceram. Soc., 85 (2002) 3036.

[8] P.D. Sarkisov, N.V. Popovich and A.G. Zhelnin, Glass and Ceramics, 60 (2003) 309.

[9] Zuoling Fu, Shihong Zhou, and Siyuan Zhang, J. Phys. Chem. B 109 (2005) 14396.

[10] Y.K.Song, S. K. Choi and H.S. Moon, Materials Research Bulletin, 32 (1997) 337.

[11] Yun Liu and Chao-Nan Xu, J. Phys. Chem. B 107 (2003) 3991.

[12] T. Matsuzawa, Y. Aoki, N. Takeuchi, Y. Murayama, J. Electrochem. Soc. (8) **143** (1996) 2670.

[13] F. Jie, Electrochem. Solid State Lett. (7) **3** (2000) 350.

[14] D. J. Vij and V. K. Mathur, Ind. J. Pure and Appl. Phys. 6, 67 (1968).

[15] F. Okamoto and K. Kato, J. Electrochem. Sot. 130,432 (1983).

[16] G. Blasse, Mat. Chem. and Phys. 16, 201 (1987).

[17] S. Asano and N. Yamashita, Phys. Stat. Sol. 197, 311 (1980).

[18] Y. Yamshita and S. Asano, M. Oshishi and K. Ohmor, Jpn. J. Phys Sot. 53, 4225 (1985).

[19] C.R. Ronda, T. Justel, H. Nikol, J. Alloys Compd. 275–277 (1998) 669.

[20] T. Justel, H. Nikol, C. Ronda, Angew. Chem. Int. Ed. 37 (1998) 3084.

[21] S. Ekambaram, K.C. Patil, J. Alloys Compd. 248 (1997) 7.

[22] S. Ekambaram, K.C. Patil, Bull. Mater. Sci. 18 (1995) 921.

[23] T. Weller, J. Lumin. 48–49 (1991) 49.

[24] Dieke Spectra and Energy Levels of Rare Earth Ions in Crystals; Interscience Publishers: New York, 1969.

[25] Reisfeld R., Gaft M., Saridarov T., Panczer G., Zelner M., Mater. Lett., 45 (2000), 154.

[26] Blasse G., Grabmaier B.C., Luminescent Materials, Springer-Verlag, Berlin, 1994, p. 41ff.

[27] M.K. Cinibulk, J. Am. Cram. Soc. 83 (2000) 1276.

[28] R.L. Calvert and R.J. Danby, Radiat. Prot. Dosim. 6 (1984) 55.

[29] R.L. Calvert and R.J. Danby, Phys. Stat. Sol.(a) 83 (1984) 597.

[30] R.Y.Wang, Journal of Luminescence, 106 (2004) 211.

[31] Shigeo Shionoya and William Yen, Phosphor handbook, CRC Press, Boca Raton, 1999 p.190.

[32] R.Jagannathan, T.R.N.Kutty, M.Kottaisamy, P.Jeyagopal, Jpn. J. Appl. Phys., 33 (1994) 6207.

[33] Phosphor Handbook, ed. S. Shionoya, W. M. Yen, CRC Press, NY (1998) 18,189,196.

[34] Morito Akiyama, Chao-Nan Xu, Kazuhiro Nonaka, and Tadahiko Watanabe, Applied Physics Letters, 73 (1998) 3046.

[35] Morito Akiyama, Chao-Nan Xu, Yun Liu, Kazuhiro Nanoka, Tadahiko Watanabe, Journal of Luminescence, 97 (2002) 13.

[36] J. L. Sommerdijik, A. Brill, J. Electrochem. Soc. **122** (1975) 952.

[37] G. Blasse, Luminescence of Inorganic Solids, ed. B. DiBartolo, Plenum Press (1978) 457.

[38] L. Ozawa, H. N. Hersh, Tech. Digest Phosphor Res. Soc. 155th Meeting (1974) (in Japanese).

[39] S. Kuboniwa, H. Kawai, T. Hoshina, The Jpn. J. Appl. Phys. **19** (1980) 1647.

[40] R. Chen and Y. Kirsh, Pergamon Press, England, First Edition 1981, p.162.

[41] P. Page, R. Ghildiyal, K.V.R. Murthy, Mater. Res. Bull. 41 (2006) 1854.